

NATIONAL AERONAUTICS AND SPACE ADMINISTRATION

PROPOSED JOURNAL ARTICLE

EFFECTS OF GRAIN SIZE ON THE TENSILE AND CREEP  
PROPERTIES OF ARC-MELTED AND ELECTRON-  
BEAM-MELTED TUNGSTEN AT 2250° TO 4140° F

by William D. Klopp, Walter R. Witzke,  
and Peter L. Raffo

Lewis Research Center  
Cleveland, Ohio

GPO PRICE \$ \_\_\_\_\_

CFSTI PRICE(S) \$ \_\_\_\_\_

Hard copy (HC) 2.00

Microfiche (MF) .50

ff 653 July 65

FACILITY FORM 606	N65-29425	
	(ACCESSION NUMBER)	(THRU)
	29	1
	(PAGES)	(CODE)
	TMX-54756	17
	(NASA CR OR TMX OR AD NUMBER)	(CATEGORY)

Prepared for

American Institute of Mining, Metallurgical, and Petroleum Engineers Transactions  
July 21, 1964

The creep behavior of powder-metallurgy tungsten has been studied, but no data are available on the creep behavior of tungsten consolidated by melting. Green<sup>(4)</sup> found that powder-metallurgy tungsten exhibited linear creep at 4082° to 5072° F with an activation energy of 160,000 cal/g mol. The similarity of this activation energy to that of 153,000 cal/(g)(mole) for volume self diffusion<sup>(5)</sup> suggests that recovery of strain-hardening by dislocation climb is rate-controlling in this temperature range.

In studies at 4800° F, Sutherland and Klopp<sup>(6)</sup> concluded that grain size significantly affected the creep behavior of commercial powder-metallurgy tungsten, the finer-grained materials being stronger than the coarse-grained materials. This grain-size effect was suggested by Sherby<sup>(7)</sup>, although the opposite relation had been generally accepted for aluminum<sup>(8)</sup> and several other materials<sup>(9,10)</sup>.

The purpose of the present study was twofold; first, to provide base-line data on high-temperature tensile and creep properties of arc-melted and EB-melted tungsten for concurrent tungsten alloy studies, and, second, to determine the phenomenological effects of structural and purity variables on the high temperature mechanical properties of tungsten.

#### EXPERIMENTAL

The arc-melted tungsten materials were prepared by melting sintered  $1\frac{1}{4}$ -inch-diameter electrodes into  $2\frac{1}{2}$ -inch-diameter by 5-inch-long ingots. The arc-melting facility has been described previously<sup>(2)</sup>. Eight ingots were melted, machined, and hot extruded at 3450° F to reductions of 6 to 1 or 8 to 1. The extruded rods were then warm swaged at 2800° to 2100° F to a final diameter of 0.36 inch.

Two ingots were prepared from similar electrode material by multiple EB-melting. An initial rapid melt was employed to consolidate the electrode into an

# EFFECTS OF GRAIN SIZE ON THE TENSILE AND CREEP

## PROPERTIES OF ARC-MELTED AND ELECTRON-BEAM-

MELTED TUNGSTEN AT 2250° TO 4140° F

by William D. Klopp, Walter R. Witzke,  
and Peter L. Raffo\*

Lewis Research Center  
National Aeronautics and Space Administration  
Cleveland, Ohio

### ABSTRACT

29425

E-2681 A study was conducted of the tensile and creep properties of arc-melted and electron-beam-melted tungsten over the temperature range 2250° to 4140° F. The tensile and creep strengths vary with grain size, the finer grained materials being stronger. The temperature dependencies for transient creep, and for steady creep, correspond to activation energies of 95,000 and 141,000 cal/(g)(mole), respectively. The magnitudes of these activation energies suggest that cross-slip is rate-controlling during transient creep, while dislocation climb is rate-controlling during steady creep.

Author

### INTRODUCTION

Although considerable data have been generated on the high temperature tensile properties of powder-metallurgy tungsten<sup>(1)</sup>, relatively few data have been published on the properties of arc-melted<sup>(2)</sup> or electron-beam-melted tungsten<sup>(3)</sup>. Further, the available data show a fairly large amount of scatter at high temperatures. The effects of structure and purity have not yet been defined, aside from an observation<sup>(3)</sup> that high-purity electron-beam(EB-)-melted tungsten is weaker than powder-metallurgy tungsten of comparable grain size.

---

\*W. D. Klopp, member AIME, W. R. Witzke, and P. L. Raffo, Junior member, AIME, are Research Metallurgists, NASA Lewis Research Center, Cleveland, Ohio.

ingot, which was then slowly remelted five or six times into a  $2\frac{1}{2}$ -inch-diameter crucible for further purification. The EB-melting facility has been described previously<sup>(3)</sup>. These two ingots were extruded at 3000° and 3500° F to a 6 to 1 reduction ratio, followed by swaging to 0.36-inch-diameter rod at temperatures 100° to 200° F lower than those used for swaging the arc-melted materials.

Chemical analyses were obtained on tungsten consolidated by the two melting processes and are given in Table I.

Specimens for both tensile and creep studies were ground from the swaged rods. The specimen reduced section was 0.16 inch in diameter by 1.03 inch long.

Tensile studies were conducted on an Instron testing machine equipped with a water-cooled stainless steel furnace which has been described previously<sup>(11)</sup>. Pressure in the furnace was maintained at  $10^{-5}$  torr during testing. The heating element was a  $1\frac{1}{2}$ -inch-diameter by 7-inch-long split tantalum sleeve. The cross-head speed during testing was 0.005 inch per minute until the apparent yield point was exceeded, after which the rate was increased to 0.05 inch per minute. Limited studies were also conducted at constant cross-head speeds of 0.002, 0.02, 0.2, and 2 inches per minute. True-stress-true-strain flow curves were constructed for each tensile test up to the point of maximum load by assuming constant volume and uniform deformation in the reduced section. Since extensometers capable of measuring specimen strain in the 2500° to 4000° F range were not available, the specimen elongation was taken as equal to the cross-head motion.

Short-time step-load creep tests were also conducted in the tensile machine. For these tests, load cycling controls allowed the load to cycle around a preset load by  $\pm\frac{1}{2}$  percent. The cross-head speed was adjusted during testing to produce minimum cycling. The loads were increased in 10-percent increments at 15-minute intervals.

Long-time creep tests were conducted in a conventional beam-load machine equipped with a vacuum chamber and tantalum heater similar to that used for tensile testing. Sample extensions were measured from loading rod movement and corrected for settling and creep of the loading rods.

Grain sizes were measured metallographically on the heated but undeformed shoulders of all tensile and creep specimens after testing by using a boundary-intercept counting method<sup>(12)</sup>.

Calibrated W/W-26Re thermocouples were used for all temperature measurements.

## RESULTS AND DISCUSSION

### Tensile Studies

High-temperature tensile data were obtained on arc-melted and EB-melted specimens in the as-swaged condition and after annealing at temperatures from 2500° to 4200° F. The data are summarized in Table II. As seen from the plot of ultimate tensile strength versus test temperature in Fig. 1, considerable variation in strength was observed at each test temperature. The as-swaged arc-melted tungsten was strongest, while annealed EB-melted tungsten was weakest.

Metallographic studies on the broken specimens suggested that these differences in strength were associated with differences in microstructure. Swaged arc-melted tungsten retained a worked structure after testing at 2500° or 3000° F, indicating that the high strengths result from retained strain-hardening. The specimens tested at 3500° or 4140° F exhibited fine and coarse-grained equiaxed structures, respectively. The swaged EB-melted specimens had equiaxed structures, after testing at 2500° F or higher, indicating a much lower recrystallization temperature for this material.

The strength variations for the swaged materials that recrystallized during testing as well as those that were annealed before testing could be correlated with grain size. A plot of ultimate and yield strength for the arc-melted specimens and ultimate strength for the EB-melted specimens versus average grain diam-

eter, presented in Fig. 2, shows that the strengths decrease with increasing grain size. The grain size dependencies, which appear to be unaffected by temperature over the range 2500° to 3500° F may be expressed as

$$\sigma_u = AL^{-0.12} \quad (1)$$

$$\sigma_y = BL^{-0.25} \quad (2)$$

where

$\sigma_u$  ultimate tensile strength, psi

$\sigma_y$  0.2 percent offset yield strength, psi

A,B temperature dependent constants

L average grain diameter, cm

Thus, decreasing the grain size from 0.1 cm, typical for arc-melted tungsten annealed above 4000° F, to 0.005 cm, typical for just-recrystallized arc-melted tungsten, increases the ultimate strength by 40 percent and the yield strength by 80 percent.

It is also apparent from Fig. 2 that the ultimate strengths of the EB-melted materials were only about 85 percent as high as the ultimate strengths of arc-melted tungsten at the same grain sizes. In view of the fairly large differences in metallic impurity contents between arc-melted and EB-melted tungsten, as shown in Table I, this difference is attributed to impurity strengthening in the arc-melted material.

Considerable scatter was observed in the yield-strength data for EB-melted tungsten, and these data could not be fitted to a straight-line relationship with grain size. The yield strengths were considerably below those exhibited by arc-melted tungsten, as seen from the data in Table II.

True stress was plotted against true strain from tensile data for the recrystallized materials to obtain the parabolic strain-hardening coefficient<sup>(13,14)</sup> from the relation

$$\chi = (\sigma - \sigma_y)^2 / \epsilon \quad (3)$$

where

$\chi$  strain-hardening coefficient,  $\text{psi}^2$

$\sigma$  true stress,  $\text{psi}$

$\epsilon$  true strain

The strength coefficient  $S$  and the strain-hardening exponent  $n$  were also obtained from log-log plots of the data according to the familiar relation

$$\sigma = S\epsilon^n \quad (4)$$

Values for the constants  $\chi$ ,  $S$ , and  $n$  are included in Table II.

Representative parabolic plots of flow curves for arc-melted tungsten are shown in Fig. 3. The experimental data at 2500° F gave good fits when plotted parabolically, but at higher temperatures, reasonable plots were only obtained at low to intermediate strains. The deviations at higher strains are attributed to grain boundary tearing and sliding, which invalidate the assumptions of constant volume and uniform deformation upon which the true stress and true strain calculations are based.

The strain-hardening coefficients decreased with increasing temperature and with increasing grain size, as seen from the data in Table II. Although the data exhibited some scatter, the grain-size dependency of the strain-hardening coefficient for arc-melted tungsten did not appear to vary with temperature and could be expressed by

$$\chi = CL^{-0.2} \quad (5)$$

where  $C$  is a temperature-dependent proportionality constant. The strain-hardening coefficients for EB-melted tungsten were much lower than would correspond to extrapolation of the data for arc-melted tungsten to larger grain sizes and, because of data scatter and few data points, could not be fitted to a grain size plot.

Log-log plots of true stress versus true strain generally gave straight lines for arc-melted tungsten, but the plots for EB-melted tungsten tended to curve upwards slightly with increasing strain. This material also exhibited higher strain-hardening exponents than did arc-melted tungsten. Data from the present study are not considered sufficiently accurate to distinguish a better fit with either the parabolic or exponential type of relation, since true strain was calculated from cross-head motion rather than true specimen elongation. The instantaneous strain-hardening rates may be calculated from the following equations, which are differentials of equations (3) and (4):

$$d\sigma/d\epsilon = \frac{1}{2}\sqrt{X/\epsilon} \quad (3a)$$

$$d\sigma/d\epsilon = nS\epsilon^{n-1} \quad (4a)$$

Sample comparisons (not shown) of the differentials calculated from equations (3a) and (4a) indicated differences up to 40 percent when the exponent  $n$  was in the range 0.25 to 0.35; for those EB-melted specimens where  $n$  approached 0.5, the instantaneous strain-hardening rates were similar at least over the strain range 0.02 to 0.2. The latter observation is in agreement with the fact that equations (3a) and (4a) are equivalent when  $n$  equals 0.5, with  $X$  equal to  $S^2$ .

Variations in strength and strain-hardening coefficients with grain size at high temperatures have been observed previously (8, 15), although a complete picture of the mechanism has not yet emerged.



A mechanism based on strain-hardening has been described by McLean<sup>(8)</sup>, who suggests that the increased strength with decreasing grain size results from the increased complexity of slip within the individual grains. During deformation of a polycrystalline material, the individual grains are partially constrained by their neighbors so that slip on a given plane can proceed only to the extent that the neighboring grains can deform to accommodate the changing grain shape. As the limit of deformation in a given direction is approached, the resolved stresses within the grain increase and slip begins on other planes more favorably oriented with respect to the neighboring grains. Decreasing grain size reduces the total strain that can be accommodated on the most favorably oriented slip planes, and the stress increases more rapidly with total strain in order to activate slip on less favorably oriented planes, giving rise to the observed increasing strength and strain-hardening rate with decreasing grain size.

A second possible explanation is concerned with the effect of grain boundaries on dislocation density. It has been shown recently<sup>(16)</sup> that the density of mobile dislocations  $\rho$  is approximately proportional to the first power of strain  $\epsilon$

$$\rho = D\epsilon^c \quad (c = \text{about } 1) \quad (6)$$

and the flow stress  $\sigma$  to produce plastic strain is proportional to the square root of the dislocation density

$$\sigma = \sigma_0 + \alpha\sqrt{\rho} \quad (7)$$

where

$\sigma_0$  stress to initiate dislocation motion, psi

$\alpha$  proportionality constant

By substituting Eq. 6 into Eq. 7, a parabolic relation between  $\sigma$  and  $\epsilon$  is obtained which is similar to Eq. 3:

$$\sigma = \sigma_0 + \alpha\sqrt{D\epsilon^c} \quad (8)$$

It is further seen that increasing the dislocation density for a given strain, i.e., increasing the proportionality factor  $D$  between  $\rho$  and  $\epsilon$ , increases the required flow stress and has the same effect as increasing the strain-hardening coefficient  $X$  in Eq. 3.

Since grain boundaries can act both as sources and multiplication sites for dislocations, an increase in the grain boundary area per unit volume (reduction in grain size) could affect the strength and strain-hardening coefficient by increasing the dislocation density for a given strain.

#### Creep Studies

Constant-load and step-load creep studies were conducted on arc-melted and EB-melted tungsten at temperatures from 2250° to 4000° F. Data from these studies are summarized in Tables III and IV.

Representative constant-load creep curves for arc-melted tungsten at 3000° F are shown in Fig. 4. The creep of tungsten at this temperature may be represented by periods of transient or primary creep, during which the creep rate decreases; steady or secondary creep, during which the creep rate remains constant; and tertiary creep, characterized by an increasing creep rate terminating in fracture. At 2750° F and lower, only transient creep was observed prior to tertiary creep, while at 2875° F and higher, both transient and steady creep were observed.

A plot of steady creep rates and approximate rupture lives versus stress at 3000°, 3500°, and 4000° F is shown in Fig. 5. The rupture life scale is calculated from the relation

$$\dot{\epsilon}t_r = \text{constant} \quad (9)$$

where

$\dot{\epsilon}$  steady creep rate,  $\text{sec}^{-1}$

$t_r$  rupture life, sec

Using a value of 0.2 for  $K$ , the average error in the rupture life scale for the data of this study is  $\pm 23$  percent. Also included are tensile data on arc-melted tungsten at strain rates of  $3.3 \times 10^{-5}$  to  $3.3 \times 10^{-2} \text{ sec}^{-1}$ . These data show considerable scatter at each temperature.

The steady creep rate data were analyzed by the method of least mean squares and fitted to a relationship of the type recently proposed by Sherby<sup>(7)</sup>:

$$\dot{\epsilon} = K \sigma_c^a L^b \quad (10)$$

where

$K$  temperature-dependent constant

$a, b$  temperature-independent constants

$\sigma_c$  engineering creep stress

Average values of 5.8 were determined for  $a$ , the exponential stress factor, and 0.43 for  $b$ , the exponential grain size factor. The stress factor of 5.8 is close to the value of 6.3 observed by Green<sup>(4)</sup> for powder-metallurgy tungsten at higher temperatures.

The grain size factor of 0.43 is less than the value of 2 proposed in the recent review by Sherby<sup>(7)</sup> and observed by Feltham and Meakin in copper<sup>(17)</sup> and Sutherland and Klopp in powder-metallurgy tungsten<sup>(6)</sup>. However, the increase in creep rate with increasing grain size is in qualitative agreement with these and other recent observations<sup>(18-20)</sup>. In contrast, studies on aluminum<sup>(8)</sup> and other metals<sup>(9,10)</sup> showed the opposite effect, the coarse-grained materials being more creep-resistant than the fine-grained materials. The reasons for these conflicting observations have not yet been satisfactorily explained.

The stress necessary to give a creep rate of  $10^{-6}\text{sec}^{-1}$  is plotted against grain size in Fig. 6. The stress during creep is proportional to the -0.074 power of grain size, as calculated from Eq. 8. This is measurably less than the exponential factor of -0.12 observed for the dependency of the short-time ultimate tensile strength on grain size (shown in Fig. 2), implying that there may be a change or modification in the rate-controlling reaction. The strength at elevated temperatures is considered to be determined from competition between strain-hardening and recovery reactions. During tensile testing, where the total time is short, strain-hardening may exert the predominant influence on strength. During creep testing, however, the test times are considerably longer and recovery reactions are considered rate-controlling. The mechanisms by which grain size is postulated to affect strength are increasing the complexity of slip and/or increasing the dislocation density. Since these are both associated with strain-hardening rather than recovery, the decrease in grain-size dependence may reflect the increasing importance of recovery as the rate-controlling reaction at low strain rates.

It is also apparent from Fig. 6 that the creep strengths of both arc-melted and EB-melted tungsten are similar when compensated for grain size; in contrast, EB-melted tungsten was weaker than arc-melted tungsten of similar grain size in short-time tensile tests. This difference in behavior suggests that impurities which moderately strengthen arc-melted tungsten during tensile testing by increasing the rate of strain-hardening are relatively ineffective during creep, further reflecting the increasing importance of recovery rather than strain-hardening as the rate-controlling reaction at low strain rates.

The steady creep rate data and the tensile strengths at various strain rates were replotted against stress (Fig. 7) after the creep rates and strengths, respectively, were normalized to a grain size of 0.04 cm, about midway in the range of grain sizes studied. The introduction of the grain size factor considerably reduces the scatter in these data. The tensile strengths are also similar to the creep strengths at similar strain rates. The change in slope of the strain rate-versus-stress plots at 3000° and 3500° F and strain rates greater than  $10^{-3} \text{ sec}^{-1}$  indicates a change in the rate-controlling reaction, possibly from recovery at the low strain rates to strain-hardening at the high strain rates.

The temperature dependency of the high-temperature creep of tungsten is shown in Fig. 8. The data of Green<sup>(4)</sup> are also shown. The lack of correlation between the data of Green and of the present study may reflect compositional differences between Green's powder metallurgy tungsten and arc- and EB-melted tungsten. At temperatures above about 3300° F, the temperature dependency corresponds to an activation energy of 141,000 cal/(g)(mole), slightly less than the 160,000 cal/(g)(mole) observed by Green. Below about 3300° F, the temperature dependency is seen to decrease.

The activation energy of 141,000 cal/(g)(mole) is close to that for self-diffusion in tungsten, 153,000 cal/(g)(mole)<sup>(5)</sup>, suggesting that recovery of strain-hardening by dislocation climb is the rate-controlling mechanism above 3300° F. The significance of the decrease in activation energy below 3300° F is not entirely clear. Cross-slip has been postulated as the rate-controlling recovery mechanism in the temperature range below that for dislocation climb, i.e., about 0.4 to 0.5  $T_m$ <sup>(8,21)</sup>. However, it is generally considered that cross-slip is not the mechanism by which edge dislocations can be recovered; thus, this mechanism cannot result in complete recovery and does not give steady creep be-

havior. It is likely that the behavior in the 2875 to 3300°F range represents a transition between climb, which recovers edge dislocations at the higher temperatures and cross-slip at the lower temperatures.

The transient or primary creep flow was also studied at 2250° to 3500° F in order to characterize more completely the high temperature creep behavior of tungsten and to determine the relation between transient and steady flow rates. The transient portions of the creep curves for annealed specimens could be correlated according to the familiar Andrade relation

$$e = \beta t^{1/3} \quad (11)$$

where

e engineering strain

t time, sec

$\beta$  transient creep rate,  $\text{sec}^{-1/3}$

Fig. 9 compares the transient creep rates with the subsequent steady creep rates at 2875° to 3500° F for both arc-melted and EB-melted material. It is seen that for EB-melted and for annealed arc-melted specimens, the rates may be correlated by a parabolic relation

$$\dot{e} = 0.3 \beta^2 \quad (12)$$

Similar relations have been observed previously for copper<sup>(16)</sup> and for columbium<sup>(22)</sup>, while data for lead<sup>(18)</sup> showed a cubic relation between  $\dot{e}$  and  $\beta$ . The transient flow for arc-melted specimens which were initially in the swaged condition was less than for annealed specimens which had similar steady creep rates and could not be fitted to the Andrade relation. Apparently the swaged specimens were strengthened by retained strain-hardening that was not recovered, at least not during the transient creep period.

The relation between transient creep rate, stress, and grain size was calculated from equations (10) and (12) as

$$\beta = K' \sigma_c^{2.9} L^{0.22} \quad (13)$$

The good fit obtained with this relation is shown in Fig. 10, where the transient creep rates, normalized to a grain size of 0.04 cm, are plotted versus stress.

The temperature dependency of the transient creep rates is shown in Fig. 11. The data over the entire temperature range studied, 2250° to 3500° F, are related by an activation energy of 95,000 cal/(g)(mole) with no apparent inflections in the curve. It is believed that this activation energy is associated with recovery by the cross-slip mechanism. It appears that below 0.5  $T_m$  (2875° F), cross-slip is the predominant recovery mechanism, so that only transient creep is observed. Above 2875° F, creep initially is probably controlled by the rate of recovery by cross-slip until, at longer times, when creep rate has diminished, the slower recovery of edge dislocations by climb can become rate-controlling.

#### CONCLUSIONS

The following conclusions are drawn from this study:

1. The ultimate and yield strength of arc-melted tungsten at 2500° to 3500° F decrease significantly with increasing grain size, the relations being  $\sigma_u = AL^{-0.12}$  and  $\sigma_y = BL^{-0.25}$ .
2. The lower tensile strength of high-purity EB-melted tungsten as compared to arc-melted tungsten is attributed primarily to the larger grain size of the EB-melted material. A smaller effect is probably associated with purity, the arc-melted tungsten being about 15 percent stronger than the EB-melted tungsten at similar grain sizes.

3. There appeared to be no difference in creep behavior between arc-melted and EB-melted tungsten except that associated with grain size. Impurities that strengthened arc-melted tungsten during tensile testing were not strengthening during creep.

4. Both the steady creep rates and the transient creep rates increase with increasing grain size. The creep relations are  $\dot{\epsilon} = K\sigma^{5.8}L^{0.43}$  and  $\beta = K'\sigma^{2.9}L^{0.22}$ , where  $\dot{\epsilon}$  and  $\beta$  are the steady and transient creep rates, respectively,  $K$  and  $K'$  are temperature-dependent constants,  $\sigma$  is stress, and  $L$  is average grain diameter.

5. The activation energy for steady creep above about 3300° F was 141,000 cal/(g)(mole); from 3300° to 2875° F it decreased. The magnitude of the activation energy suggests that dislocations climb is rate-controlling above 3300° F. The activation energy for transient creep at 2250° to 3500° F was 95,000 cal/(g)(mole); it is suggested that cross-slip is the rate-controlling reaction during transient creep.

#### REFERENCES

1. J. L. Ratliff, and H. R. Ogden: A Compilation of the Tensile Properties of Tungsten, DMIC. Memo. 157, Sept. 11, 1962.
2. F. A. Foyle: Arc-Melted Tungsten and Tungsten Alloys, High Temperature Materials II, Interscience, New York, 1963.
3. W. R. Witzke, E. C. Sutherland, and G. K. Watson: Preliminary Investigation of Melting, Extruding, and Mechanical Properties of Electron-Beam-Melted Tungsten, NASA TN D-1707, 1963.
4. W. V. Green: Short-Time Creep-Rupture Behavior of Tungsten at 2250° to 2800° C, Trans. AIME, 1959, vol. 215, p. 1057.



5. R. L. Andelin: Self-Diffusion in Single-Crystal Tungsten and Diffusion of Rhenium Tracer in Single-Crystal Tungsten, Los Alamos Report LA 2880, April 22, 1963.
6. E. C. Sutherland, and W. D. Klopp: Observations of Properties of Sintered Wrought Tungsten Sheet at Very High Temperatures, NASA TN D-1310, 1963.
7. O. D. Sherby: Factors Affecting the High Temperature Strength of Polycrystalline Solids, Acta Met., 1962, vol. 10, p. 135.
8. D. McLean: Mechanical Properties of Metals, John Wiley, New York, 1962. pp. 122; 307.
9. A. H. Sully: Metallic Creep and Creep-Resistant Alloys, Interscience, New York, 1949.
10. C. L. Clark: High-Temperature Alloys, Pitman, London, 1953.
11. P. F. Sikora, and R. W. Hall: High-Temperature Tensile Properties of Wrought Sintered Tungsten, NASA TN D-79, 1959.
12. Standard Methods for Estimating the Average Grain Size of Metals, 1961 ASTM Standards, Part 3, ASTM, Philadelphia, 1961.
13. L. M. Clarebrough, and M. E. Hargreaves: Work Hardening of Metals, Progress in Metal Physics, Vol. 8, Pergamon Press, New York, 1959, p. 93.
14. R. J. Wasilewski: On Discontinuous Yield and Plastic Flow in  $\alpha$ -Titanium, ASM Trans., 1963, vol. 56, p. 221.
15. M. Gensamer: The Effect of Grain Boundaries on Mechanical Properties, Relation of Properties to Microstructure, ASM, Cleveland, 1954.
16. A. S. Keh, and S. Weissmann: Deformation Substructure in Body-Centered-Cubic Metals, The Impact of Transmission Electron Microscopy on Theories of the Strength of Crystals, Interscience, New York, 1962.

17. P. Feltham, and J. D. Meakin: Creep in Face-Centred Cubic Metals with Special Reference to Copper, Acta Met., 1959, vol. 7, p. 614.
18. P. Feltham: On the Mechanism of High-Temperature Creep in Metals with Special Reference to Polycrystalline Lead, Proc. Phys. Soc., 1956, vol. B69, p. 1173.
19. High-Temperature Materials Program Progress Report No. 23, Part A, G. E. Report GEMP-23A, Contract AT (40-1)-2847, May 31, 1963.
20. E. R. Parker: Modern Concepts of Flow and Fracture, ASM Trans., 1958, vol. 50, p. 52.
21. P. R. Landon, J. L. Lytton, L. A. Shepard, and J. E. Dorn: The Activation Energies for Creep of Polycrystalline Copper and Nickel, ASM Trans., 1959, vol. 51, p. 900.
22. G. Brinson, and B. B. Argent: The Creep of Niobium, J. Inst. Metals, 1962-1963, vol. 91, p. 293.

TABLE I. - ANALYSES OF TEST MATERIALS

Element	Amount detected, ppm	
	Arc-melted tungsten (average of five ingots)	Electron-beam-melted tungsten (after two remelts)
Oxygen	$5 \pm 2$	$3 \pm 1$
Nitrogen	$10 \pm 2$	$6 \pm 1$
Carbon	$6 \pm 1$	$6 \pm 3$
Hydrogen	<1	<1
Aluminum	$9 \pm 5$	<2
Iron	$25 \pm 15$	2
Molybdenum	15	1
Nickel	$4 \pm 3$	<2
Silicon	$10 \pm 2$	<3

TABLE II. - HIGH-TEMPERATURE TENSILE PROPERTIES OF ARC-MELTED AND ELECTRON-BEAM-MELTED TUNGSTEN

Test temperature, °F	Annealing conditions		0.2 Percent offset yield strength, psi	Ultimate tensile strength, psi	Elongation, percent	Reduction in area, percent	Strain-hardening coefficient <sup>a</sup> , 10 <sup>8</sup> psi <sup>2</sup>	Strain hardening exponent <sup>b</sup> , n	Strength coefficient <sup>b</sup> , S, psi	Average grain diameter, L, 10 <sup>-3</sup> cm
	Time, hr	Temperature, °F								
Arc-melted, lot B										
2500	(c)	(c)	31,200	34,000	23.2	>95	----	----	----	(W) <sup>d</sup>
3000	1	3000	9,180	23,800	57.4	>95	22	0.310	49,000	4.5
	1/4	1800	5,700	15,460	61.5	90.5	12	.315	32,600	5.8
3500	1	2800	4,700	14,500	70.9	93.7	12	.315	30,300	5.6
	1/4	1800	4,500	10,230	75.4	91.4	5.0	.307	21,500	6.7
4140	1	2800	3,830	10,300	76.0	92.5	5.5	.324	22,200	6.4
	4	4200	2,220	7,750	62.9	>95	3.3	.326	16,000	64
	1/4	1800	1,500	4,300	73.1	>95	1.3	.331	10,000	25
	1	2800	1,400	4,700	62.6	>95	1.7	.338	11,100	25
Arc-melted, lot C										
2500	(f)	(f)	14,280	25,350	30	90.5	----	----	----	(W)
3000	(c)	(c)	24,400	36,000	20.3	95.0	----	----	----	(W)
	1	3600	6,420	18,500	57.7	>95	12	0.365	38,600	43
3500	(f)	(f)	8,620	16,910	47.8	61.7	----	----	----	(W)
	(c)	(c)	18,720	25,100	17.7	83.6	----	----	----	(W)
	1	3600	3,940	11,920	38.4	>95	6.4	.387	27,500	641
	(c)	(c)	4,150	10,270	78.9	87.6	----	.242	18,500	9.3
	1	3600	2,880	8,030	69.2	>95	3.0	.269	15,200	39
	1	3800	2,760	7,880	56.3	>95	3.0	.323	16,300	46
	1	4000	2,690	7,430	61.2	>95	2.5	.303	14,900	96
	1	4100	2,220	7,760	59.1	>95	3.4	.302	14,800	93
4	4200	2,360	7,500	61.4	>95	3.1	.320	15,500	108	
Arc-melted, lot D										
3000	(c)	(c)	10,200	15,800	49.8	88.9	----	----	----	(W)
	1	2900	17,900	23,400	41.2	>95	----	----	----	(W)

TABLE II. - Concluded. HIGH-TEMPERATURE TENSILE PROPERTIES OF ARC-MELTED AND ELECTRON-

## BEAM-MELTED TUNGSTEN

Test temperature, $T_F$	Annealing conditions		0.2 Percent offset yield strength, psi	Ultimate tensile strength, psi	Elongation, percent	Reduction in area, percent	Strain-hardening coefficient <sup>a</sup> , $10^8 \text{ psi}^2$	Strain-hardening exponent <sup>b</sup> , n	Strength coefficient <sup>b</sup> , S, psi	Average grain diameter, $L$ , $10^{-3} \text{ cm}$
	Time, hr	Temperature, $T_F$								

## Arc-melted, lot E

2500	(c)	(c)	34,700	48,000	16.2	94.3	-----	-----	-----	(W)
	1	3600	10,140	24,450	61.0	94.6	21	0.324	49,400	5.2
3000	(c)	(c)	7,650	16,200	74.5	94.0	-----	.245	30,300	3.5
	1	3600	5,430	15,770	80.2	94.8	11	.283	30,500	4.9
3500	(c)	(c)	4,140	10,570	77.2	95.6	5.4	.265	20,900	4.3
	1	3600	4,090	10,240	76.4	95.3	4.4	.248	18,500	5.3

## Electron-beam-melted, lot EB-1

2500	1	3600	5,580	16,200	59.4	>95	6.5	.278	30,000	64.4
3000	1	3600	3,750	10,300	75.2	>95	3.1	.308	20,700	99.2
3500	1	3600	920	6,210	66.7	>95	1.3	.280	12,000	127

## Electron-beam-melted, lot EB-2

2500	(c)	(c)	5,240	16,750	54.6	>95	-----	.387	36,000	30.4
	1	2500	5,050	17,100	61.2	>95	12	.363	36,200	16.6
	1	3600	2,160	12,850	30.5	>95	13	.579	35,500	188
3000	(c)	(c)	2,550	11,120	57.6	>95	-----	.452	28,900	26.2
	1	3600	1,570	7,250	25.2	>95	4.7	.583	22,600	8185
3500	(c)	(c)	860	6,220	55.9	>95	1.6	.294	13,000	129
	1	3600	990	5,870	35.6	>95	2.2	.458	14,800	183
4000	(c)	(c)	790	3,875	65.8	>95	1.2	.483	11,300	225

<sup>a</sup>Strain-hardening coefficient, X, determined from relation:  $X = (\sigma - \sigma_y)^2 / \epsilon$ .<sup>b</sup>Strain-hardening exponent, n, and strength coefficient, S, determined from relation:  $\sigma = S\epsilon^n$ .<sup>c</sup>As swaged.<sup>d</sup>W indicates fully or partially worked microstructure.<sup>e</sup>Tested at 0.002/0.02 in./min crosshead speed; all others tested at 0.005/0.05 in./min crosshead speed.<sup>f</sup>As extruded.<sup>g</sup>Estimated grain size.

TABLE III. - CONSTANT-LOAD CREEP-RUPTURE DATA AT 3000° AND 3500° F

Annealing conditions,		Test temperature, °F	Load, psi	Transient creep rate, 10 <sup>-3</sup> sec <sup>-1/3</sup>	Steady creep rate, 10 <sup>-6</sup> sec <sup>-1</sup>	Rupture life, min	Total elongation, percent	Reduction in area, percent	Average grain diameter, 10 <sup>-3</sup> cm
Time, hr	Temperature, °F								
Arc-melted, Lot A									
1	4100	3500	2,300	0.381	0.343	<sup>a</sup> 6,100	----	----	92
			3,020	-----	1.43	1,486	30.8	>98	187
			5,150	-----	72.1	35.9	32.3	>98	182
1	4200	3500	1,980	.690	.131	<sup>b</sup> 6,785	----	----	-----
			2,470	-----	.742	<sup>c</sup> 9,168.5	22.0	14.0	146
			3,040	-----	1.43	1,191.3	44.1	15.1	70
			5,040	-----	20.3	189.2	22.4	31.8	137
Arc-melted, Lot E									
(f)	(f)	3000	7,240	-----	1.79	2,673.1	81.2	85.4	7.3
			11,210	-----	<sup>d</sup> 3.62-9.8	429.2	62	93	5.3
1	4100	3000	4,760	1.50	.507	6,541.8	44.2	35.9	16.6
			6,010	4.26	3.37	1,353.6	63.8	52.6	9.6
			7,390	5.36	13.5	257.7	40.6	>98	19.5
(f)	(f)	3500	2,980	-----	.637	4,790.4	35.8	32.7	5.6
			5,130	-----	6.14	714.6	61.5	61.7	5.5
1	4100	3500	2,400	.864	.215	<sup>e</sup> 3,800	9	4.6	12.7
			3,580	-----	2.32	1,207.2	31.7	66.2	11.5
Electron-beam-melted, Lot EB-1									
1	3600	3500	2,130	0.877	0.373	10,138.8	76.4	>98	149
			4,760	12.9	80	44.8	83	>98	420

<sup>a</sup>Estimated rupture life.<sup>b</sup>Load increased to 2470 psi.<sup>c</sup>Total life including time at 1980 psi.<sup>d</sup>Rate increased from  $3.62 \times 10^{-6}$  to  $9.8 \times 10^{-6}$  after 100 min.<sup>e</sup>Test discontinued.<sup>f</sup>As swaged.

TABLE IV. - STEP-LOAD CREEP DATA AT 2250° TO 4000° F

Test tem- per- ature, °F	Annealing conditions,		Load, psi	Transient creep rate, $10^{-3}$ sec $^{-1/3}$	Steady creep rate, $10^{-6}$ sec $^{-1}$	Average grain diameter, $10^{-3}$ cm
	Time, hr	Tem- per- ature, °F				

## Arc-melted, Lot D

3500	1	3600	5,020	--	15.7	-----
			5,480	--	19.7	-----
			5,990	--	30	-----
			6,540	--	52.6	-----
3500	1	3800	6,970	--	96.6	7.21
			4,490	--	10.7	-----
			5,030	--	15.3	-----
			5,490	--	21.4	-----
			5,970	--	30.7	-----
			6,490	--	55	-----
			6,990	--	110	10.5

## Arc-melted, Lot F

3000	1	4000	7,980	--	26.3	-----
			8,970	--	40	-----
			10,080	--	84	-----
			10,980	--	210	32.2
3500	1	4000	4,720	--	19.5	-----
			5,530	--	36.2	-----
			6,220	--	68.8	-----
			6,940	--	171	38.3
3500	1	4000	5,030	--	25	-----
			5,530	--	35	-----
			6,000	--	60	-----
			6,480	--	115	32.6
4000	1	4000	2,600	--	18.3	-----
			2,890	--	26.7	-----
			3,180	--	41.2	-----
			3,490	--	73.4	29.7

TABLE IV. - CONCLUDED. STEP-LOAD CREEP DATA

AT 2250° TO 4000° F

Test temperature, °F	Annealing conditions,		Load, psi	Transient creep rate, $10^{-3}$ sec $^{-1/3}$	Steady creep rate, $10^{-6}$ sec $^{-1}$	Average grain diameter, $10^{-3}$ cm
	Time, hr	Temperature, °F				

Arc-melted, Lot G

3000	1	4200	7480	-----	43.4	-----
			8470	-----	81.3	-----
			9500	-----	200	114
4000	1	4200	2310	-----	21.7	-----
			2590	-----	30	-----
			2880	-----	50.3	-----
			3180	-----	93.3	97.6

Electron-beam-melted, Lot EB-2

2500	1/2	3000	4660	0.438	-----	-----
			5760	1.13	-----	-----
			6870	1.71	-----	37.7
3000	(a)	(a)	4010	(b)	(b)	-----
			4860	-----	4.68	87.6
3500	(a)	(a)	2450	1.46	.675	-----
			2820	-----	1.83	-----
			3185	-----	3.89	-----
			3675	-----	9.79	-----
			4165	-----	21.0	223
2250	1	3600	6200	.786	-----	-----
2500			6200	2.56	-----	-----
2750			6200	4.48	-----	205
2750	1	3600	4220	1.47	-----	-----
2875			4220	2.42	.808	-----
3000			4220	-----	1.70	-----
3125	1	3600	4220	-----	3.50	-----
3250			4220	-----	9.81	176
3525			3200	4.36	5.43	-----
3630			3200	-----	18.1	-----
3355			3200	-----	1.65	-----
3495			3200	-----	5.51	181

<sup>a</sup> As swaged<sup>b</sup> Abnormal behavior



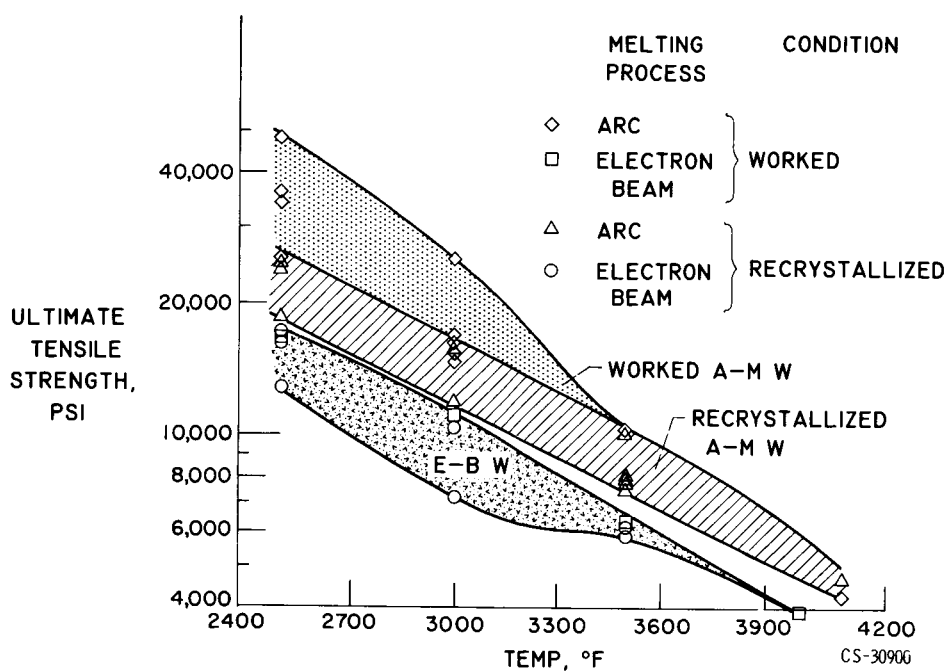


Fig. 1. - Tensile strength of arc-melted and electron-beam melted tungsten at 2500 to 4140 F.

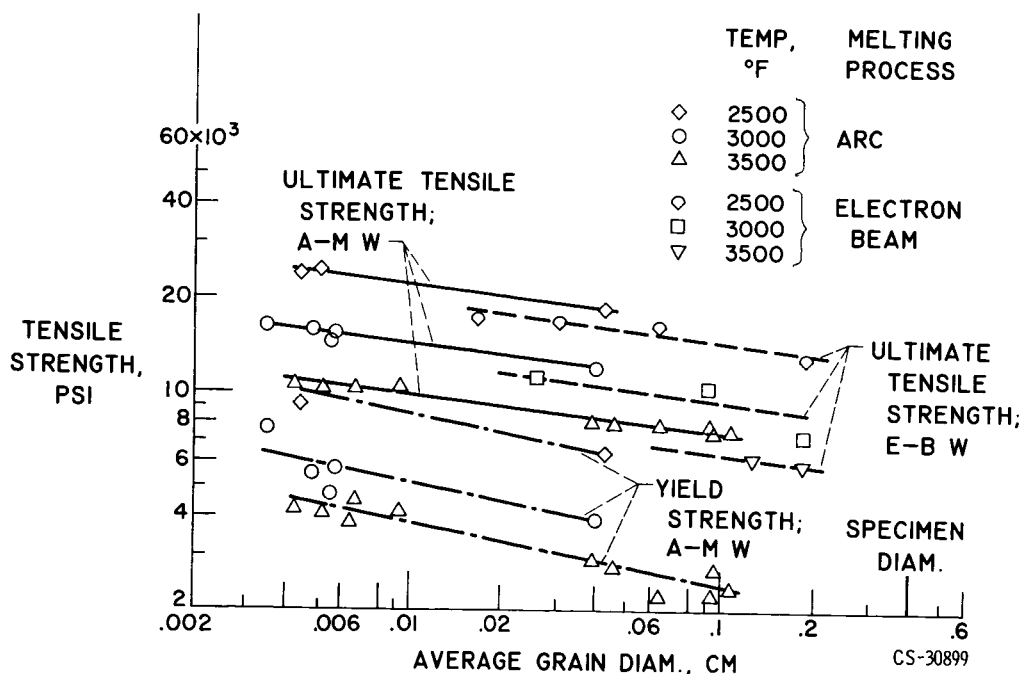


Fig. 2. - Yield and ultimate tensile strengths of arc-melted tungsten and ultimate tensile strength of electron-beam-melted tungsten as a function of grain size.

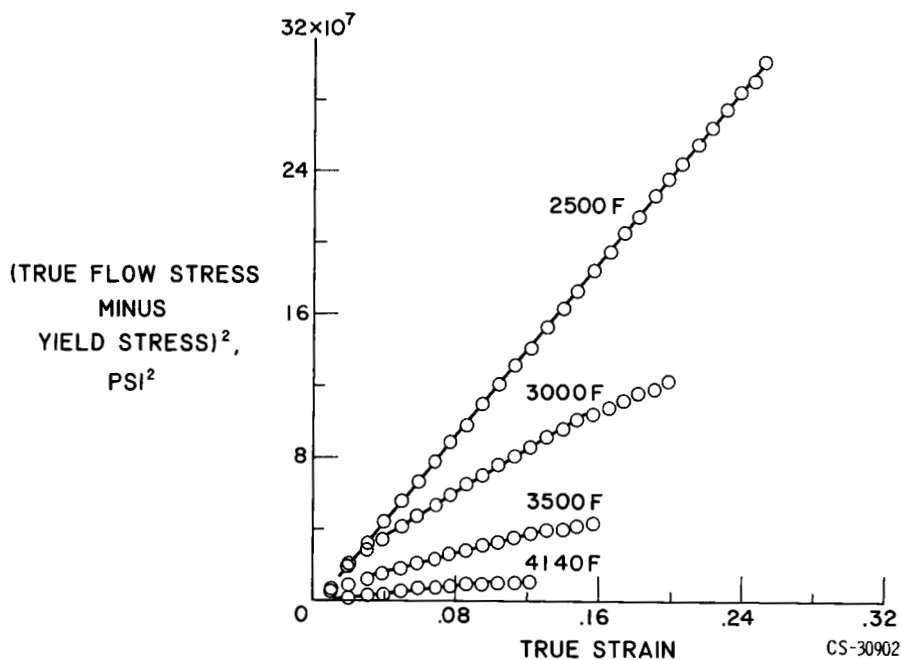


Fig. 3. - Parabolic plot of true-stress - true-strain curves for annealed arc-melted tungsten.

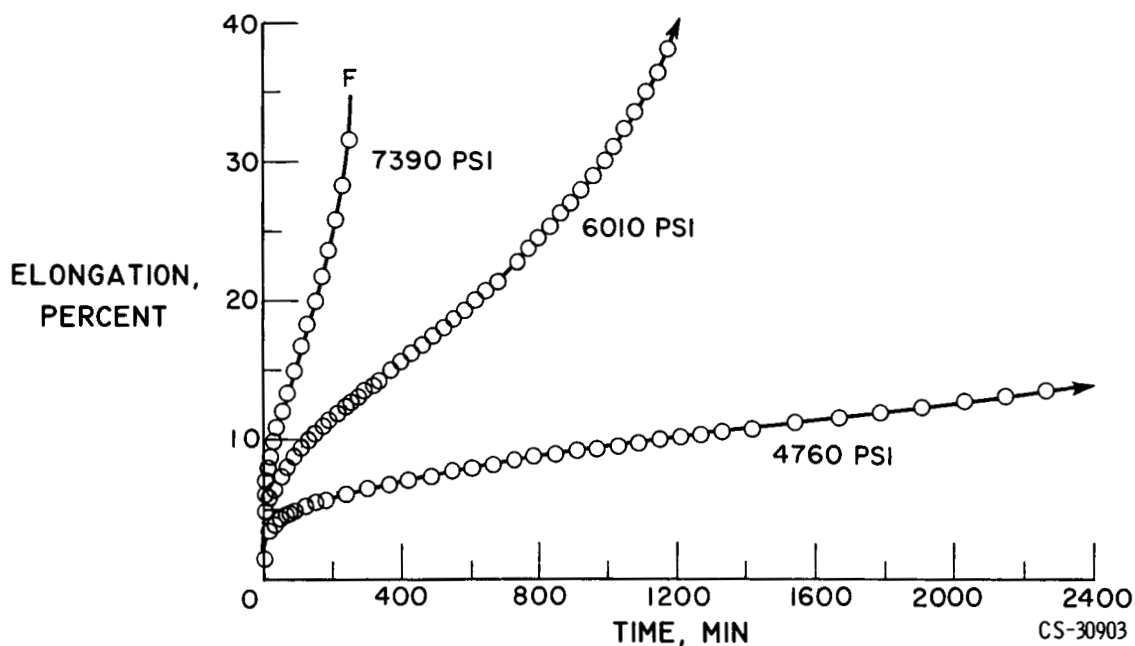


Fig. 4. - Representative creep curves of annealed arc-melted tungsten at 3000 F. (annealed for 1 hr at 3600 F; average grain diameter, 0.015 cm).

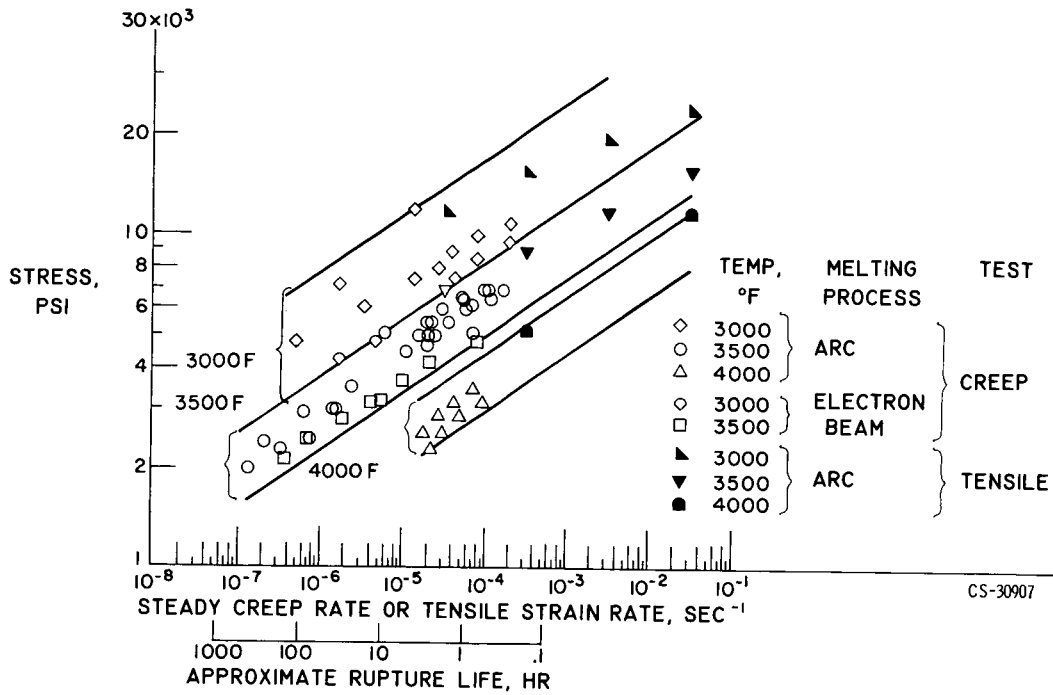


Fig. 5. - Steady creep rate as a function of stress, illustrating range of data.

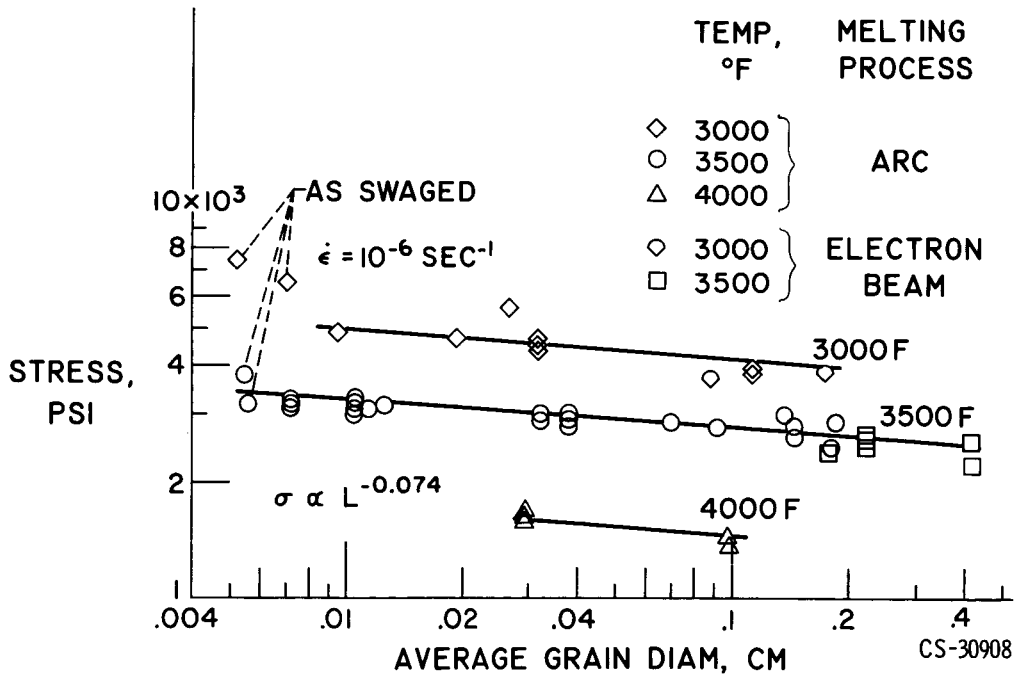


Fig. 6. - Grain size dependency of stress for a steady creep rate of  $10^{-6} \text{ sec}^{-1}$ .

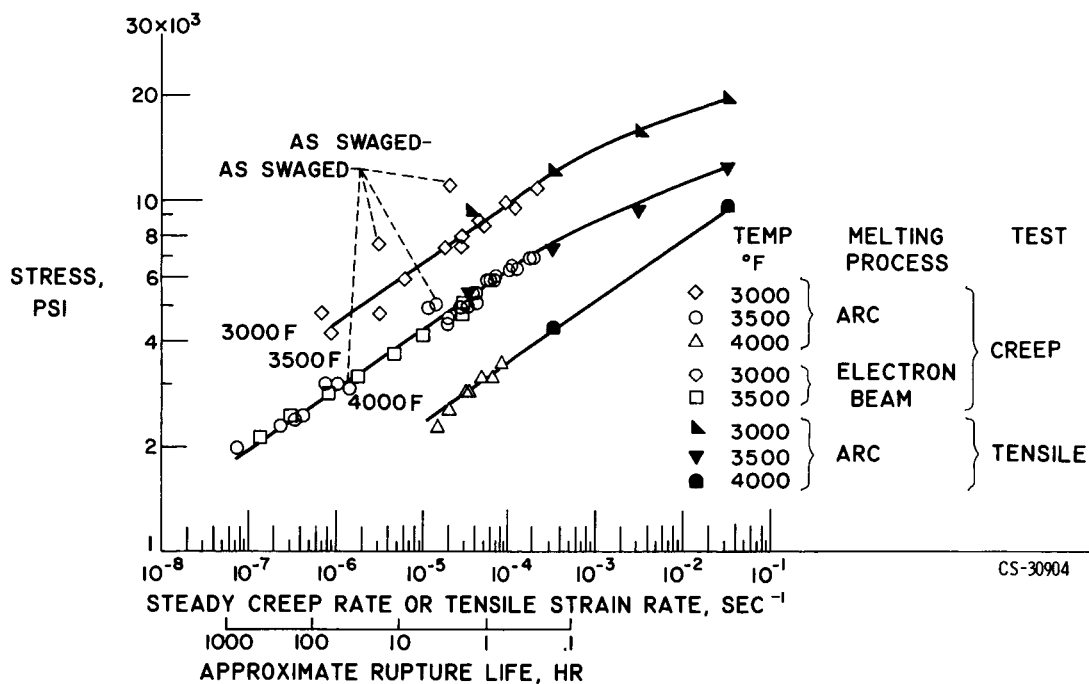


Fig. 7. - Steady creep rate as a function of stress, normalized to a grain size of 0.04 cm.

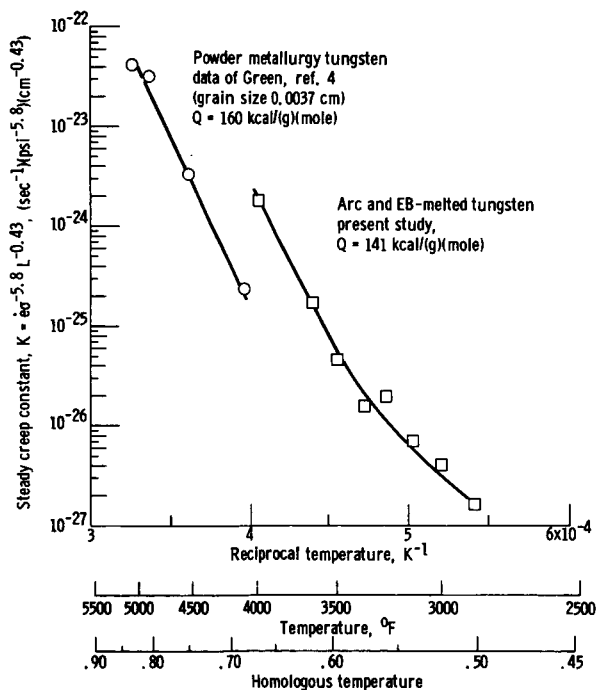


Fig. 8. - Temperature dependence of steady creep constant.

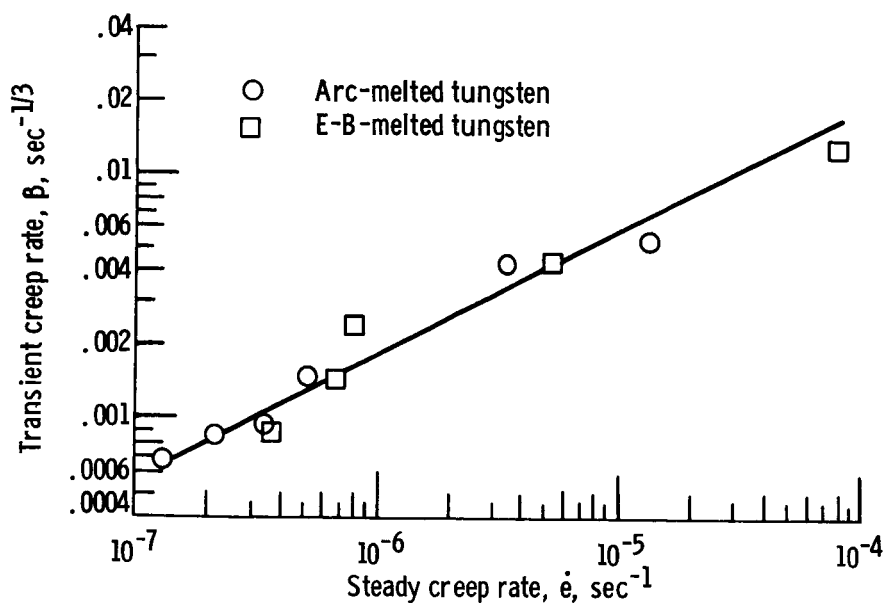


Fig. 9. - Relation between transient and steady creep rates for tungsten at 2875° to 3500° F.

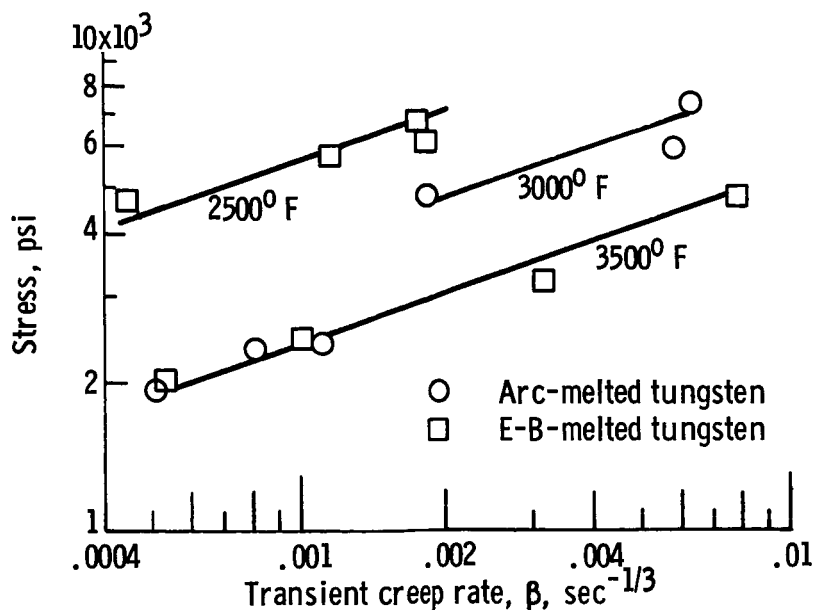


Fig. 10. - Transient creep rate as function of stress normalized to grain size of 0.04 centimeter.

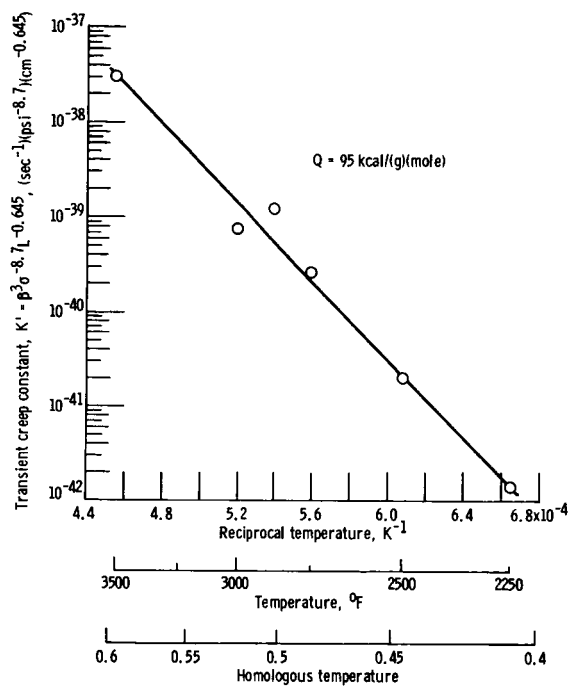


Fig. 11. - Temperature dependency of transient creep constant.